Hindawi
Advances in Condensed Matter Physics
Volume 2021, Article ID 6619252, 7 pages
https://doi.org/10.1155/2021/6619252

Research Article

First-Principles Study of Structure, Elastic Properties, and Thermal Conductivity of Monolayer Calcium Hydrobromide

Si-Hua Li,[1] Cui-E Hu,[2] Xiao-Lu Wang ,[1] and Yan Cheng[3]

[1]*School of Physics and Electronic Science, Guizhou Normal University, Guiyang 550000, China*
[2]*College of Physics and Electronic Engineering, Chongqing Normal University, Chongqing 400047, China*
[3]*College of Physics, Sichuan University, Chengdu 610064, China*

Correspondence should be addressed to Xiao-Lu Wang; wangxiaolu@gznu.edu.cn

Received 22 October 2020; Revised 18 January 2021; Accepted 1 February 2021; Published 17 February 2021

Academic Editor: Ram N. P. Choudhary

In recent years, some laboratories have been able to prepare calcium hydrobromide (CaHBr) by melting hydride and anhydrous bromide or metal and bromide in a hydrogen atmosphere at 900°C and have studied some of its properties. But there are few theoretical studies, especially the theoretical studies of monolayer CaHBr. We use the first-principles method to calculate the structure, elastic properties, and lattice thermal conductivity of the monolayer CaHBr based on the Boltzmann transport equation. We obtain a stable crystal structure by the optimization of monolayer CaHBr. By calculating the elastic constant of monolayer CaHBr, its mechanical stability is proved, and the elastic limit of monolayer CaHBr is obtained by biaxial tensile strain on monolayer CaHBr. And the corresponding phonon spectra show no imaginary frequency, indicating the dynamic stability of the monolayer CaHBr. By the ShengBTE code, we calculate the lattice thermal conductivity of the monolayer CaHBr, the iterative solution of BTE and RTA at 300 K–1200 K is obtained, and the lattice thermal conductivity at room temperature is $\kappa_l^{\mathrm{BTE}} = 2.469\ \mathrm{W/m \cdot K}$ and $\kappa_l^{\mathrm{RTA}} = 2.201\ \mathrm{W/m \cdot K}$, respectively. It can be seen that the lattice thermal conductivity of monolayer CaHBr is low. And by analyzing the phonon spectrum, the scattering rate, and the mean free path of the phonons, the lattice thermal conductivity of monolayer CaHBr mainly depends on the acoustic modes. We hope this study can provide theoretical guidance for the experiments and practical application of monolayer CaHBr.

1. Introduction

Graphene's discovery broke the prediction that two-dimensional (2D) crystalline materials could not exist stably at finite temperatures [1–6]. Various 2D materials are limited in 2D plane because of carrier migration and heat diffusion. It has made the materials exhibit many strange properties and has attracted extensive attention [7–11]. In recent years, some scholars began to pay attention to the monolayer calcium hydrobromide (CaHBr) [12–14], which can be prepared by melting hydride with anhydrous bromide [15] or metal with bromide in a hydrogen atmosphere at 900°C [14].

The hydride ion-conducting electrolytes can be used for the electrochemical detection of hydrogen in the liquid sodium coolant of fast reactors. Some laboratories discovered that the $CaBr_2$-CaHBr system has a solid electrolyte that conducts hydride ions, which can be used to develop an electrochemical hydrogen meter, and the system will show a eutectic reaction between $CaBr_2$ and CaHBr at 576°C [13]. In 1996, de Castro Vítores et al. [12] obtained the bond energy of Ca-HBr complex from independent cross molecular beam and van der Waals spectroscopy experiments. Very recently, Kumar et al. [15] measured the molar heat capacities of bulk CaHBr via the differential scanning calorimetry. It can be seen that some properties of bulk CaHBr have been studied in experiments, but there are few theoretical studies on them, especially the thermal transport properties of monolayer CaHBr.

The monolayer CaHBr is a nonmagnetic wideband gap semiconductor whose heat carriers are electrons and phonons, in which phonons dominate the heat transfer. The

lattice thermal conductivity is a key parameter for the thermal transport of semiconductors and insulators [16–19]. Peierls proposed the lattice thermal conductivity of semiconductors [20] and insulators could be described at the micros level using the phonon Boltzmann transport equation (BTE) [21]. Since then, many methods have been found to calculate the thermal conductivity of materials, such as relaxation time approximation (RTA) [22] and Callway's model [23, 24], where RTA contradicts inelastic scattering processes in principle, and the required parameters in the Callway model can only be obtained by fitting the experimental data [25]. Therefore, these methods have corresponding limitations.

As is known, ShengBTE code [26] can be used to obtain the crystal lattice thermal conductivity by solving the Boltzmann transport equation based on the force constants between harmonic and anharmonic atoms calculated from the first-principles [27]. To date, ShengBTE code has been successful to obtain the thermal conductivity and related physical quantities of many materials [28–33]. In this work, we will use the ShengBTE code to calculate the thermal conductivity of monolayer CaHBr, hoping to provide the reference value for the future experiments and theories.

2. Theoretical Methods and Calculation Details

The crystal structure is optimized by using the Vienna Ab initio Simulation Package (VASP) [34, 35] based on density functional theory. The Perdew–Burke–Ernzerhof (PBE) functional under the generalized gradient approximation (GGA) is selected as the exchange correlation functional [36, 37]. In order to eliminate the layer to layer interaction, we use a 25.32 Å vacuum layer. We use the cutoff energy of the plane wave to be 600 eV, the energy convergence of the electron relaxation to 10^{-8} eV, and a $8 \times 8 \times 1$ Monkhorst–Pack grid of k-point sampling for structural optimization. The optimized unit lattice is expanded to a supercell of $3 \times 3 \times 1$, and then, the second-order harmonic force constants (harmonic IFCs) and the third-order anharmonic force constants (anharmonic IFCs) are calculated by using Phonopy software and ShengBTE, respectively. And using the Phonopy software package can also get the phonon frequency.

There have been many studies detailing the calculation of lattice thermal conductivity using ShengBTE code [25, 26, 30, 31]; so here, we just briefly introduce this method. The resulting linearized phonon BTE when the scattering source is only two-phonon and three-phonon processes can be written as

$$F_\lambda = \tau_\lambda^0 (\nu_\lambda + \Delta_\lambda), \tag{1}$$

where τ_λ^0 is the relaxation time of mode λ, as obtained from perturbation theory. As a matter of fact, setting all Δ_λ to zero is equivalent to working within the RTA. The three-phonon scattering rates can be expressed as $\omega_j(\mathbf{q}) \pm \omega_{j'}(\mathbf{q}') = \omega_{j''}(\mathbf{q}'')$; $\mathbf{q} \pm \mathbf{q}' = \mathbf{q}'' + \mathbf{G}$, where $\omega_j(\mathbf{q})$ is the phonon frequency of mode $(j, \mathbf{q})$, and normal process correspond to $\mathbf{G} = 0$, while Umklapp processes correspond to $\mathbf{G} \neq 0$.

The lattice thermal conductivity κ_l can be obtained in terms of $\mathbf{F}$ as

$$\kappa_l^{\alpha\beta} = \frac{1}{\kappa_B T^2 \Omega N} \sum_\lambda f_0 (f_0 + 1) (\hbar\omega_\lambda)^2 v_\lambda^\alpha F_\lambda^\beta, \tag{2}$$

where Ω is the unit cell volume. In the approach implemented in ShengBTE, equation (2) is starting with a zeroth-order approximation $F_\lambda^0 = \tau_\lambda^0 \nu_\lambda$. The stopping criterion is that the relative change in the calculated conductivity tensor is less than a configurable parameter. Stopping at the zeroth iteration is equivalent to operating under the RTA. In addition, many physical quantities can also be calculated by ShengBTE code, such as the scalar mean free path Λ_λ for mode λ.

$$\Lambda_\lambda = \frac{\mathbf{F}_\lambda \cdot v_\lambda}{|v_\lambda|}. \tag{3}$$

3. Results and Discussion

3.1. Structure and Elastic Properties. The initial structure of the monolayer CaHBr is obtained from the bulk CaHBr belonging to the orthogonal structure (P4) crystal. In order to obtain the equilibrium geometric structure of monolayer CaHBr, we use the GGA method to calculate the lattice constant a and obtain the total energy E and the corresponding cell volume V; the energy-volume (E-V) data are then fitted to the Vinet equation [29]. Thus, we obtain the equilibrium lattice constant $a = 3.843$ Å, which is well consistent with another theoretical value $a = 3.829$ Å [38].

The elastic constants C_{ij} of materials are the critical significance physical quantity to measure the mechanical energy and important parameter to reflect the mechanical properties of materials [39–41]. Thus, the calculation of the elastic constant C_{ij} is of great significance for the measurement of the elastic limit of the lattice under external stress. We can calculate the elastic constants C_{ij} of two-dimensional materials by using the related theory of bulk elastic constants. In Table 1, we list the calculated elastic constants C_{11}, C_{22}, C_{12}, and C_{66}, which can be used to obtain the layer modulus γ_0, Young's modulus Y^{2D} under the Cavendish coordinates (its directions [10] and [01] in 2D materials), and Poisson's ratio ν [42, 43].

$$\gamma_0 = \frac{1}{4}(C_{11} + C_{22} + 2C_{12}), \tag{4}$$

$$Y_{10}^{2D} = Y_{01}^{2D} = \frac{C_{11}C_{12} - C_{12}^2}{C_{22}}, \tag{5}$$

$$\nu_{10} = \nu_{01} = \frac{C_{12}}{C_{11}}. \tag{6}$$

The monolayer CaHBr satisfies the stability criterion, which can be expressed by four necessary and sufficient conditions for the determination of mechanical stability [40, 41]: $C_{11} > 0$, C_{66} (the bulk material is C_{44}) > 0,

Table 1: Elastic constants C_{ij} (Nm^{-1}) and shear modulus G^{2D}, layer modulus γ_0, Young's modulus Y^{2D}, Poisson's ratio ν, the ratio of layer modulus, and sheer modulus (γ_0/G_{2D}) for the monolayer CaHBr.

Elastic properties	Our results
C_{11}	64.11
C_{22}	64.11
C_{12}	5.23
$C_{66} = G_{2D}$	17.98
$\gamma_0/\mathrm{Nm}^{-1}$	34.67
$Y^{2D}_{[10]}/\mathrm{Nm}^{-1} = Y^{2D}_{[01]}/\mathrm{Nm}^{-1}$	63.69
$\nu_{[10]} = \nu_{[01]}$	0.082
γ_0/G_{2D}	1.928

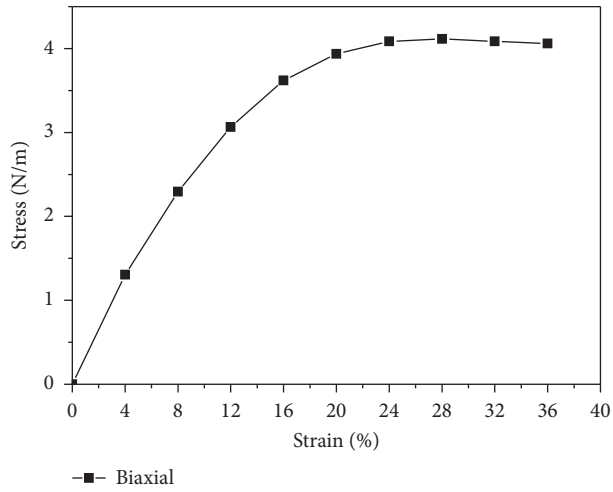

Figure 1: The relationship between biaxial strains and pressures of monolayer CaHBr.

$C_{11} > |C_{12}|, C_{11} + 2C_{12} > 0$ [44, 45]. Therefore, the monolayer CaHBr is mechanically stable. And from the elastic constant of monolayer CaHBr, it can be seen that it is smaller than that of graphene and MoS_2 [43, 46], indicating that it is a two-dimensional material with weaker hardness.

The stress-strain curve can be used to estimate the elastic limit of monolayer CaHBr. In the calculation, since the lattice constants of CaHBr on the x-axis and y-axis are the same, the corresponding biaxial tensile strain is made, as shown in Figure 1. It is our biaxial stress-strain curve. It can be seen from Figure 1 that the maximum stress that monolayer CaHBr can withstand under biaxial conditions is 4.11 N/m, which corresponds to a strain of 28%. Compared with other two-dimensional materials, monolayer CaHBr has weaker tensile capacity [32, 42].

3.2. Phonon Spectra and Scattering Rates. We calculated the phonon dispersion curves of monolayer CaHBr in Figure 2(a) together with the main view and side view of the primitive unit cell for the monolayer CaHBr (Figure 2(b)). It is shown that there is no imaginary frequency in the high symmetry directions of the phonon spectra, which indicates its dynamic stability [25, 47].

In Figure 3, we illustrate the contributions of the phonon modes to total lattice thermal conductivity at room temperature. The phonon acoustic branches clearly dominate the lattice thermal conductivity of the monolayer CaHBr, while the contribution from the optical branches is quite small. Although the contribution of the optical branch is small, the optical branch provides a scattering channel for the acoustic mode, resulting in the three-phonon scattering. So, the contribution of the optical branches cannot be ignored [29, 48].

The total converged phonon scattering rates of the monolayer CaHBr at room temperature are illustrated in Figures 4 and 5, which are corresponding to the acoustic modes and the optic modes, respectively. We notice that there is a gap between the acoustic and optical branches, consistent with that of the phonon spectra in Figure 2(a). The phonon scattering rate of the three acoustic branches is much smaller than that of the optical branch, from which it can be seen that the acoustic branch mainly contributes to the thermal conductivity of this material.

3.3. Phonon Mean Free Path and Thermal Conductivity. By calculating the phonon mean free path (MFP), we can understand how the material size affects the thermal conductivity. In Figure 6, we show the functional relationship

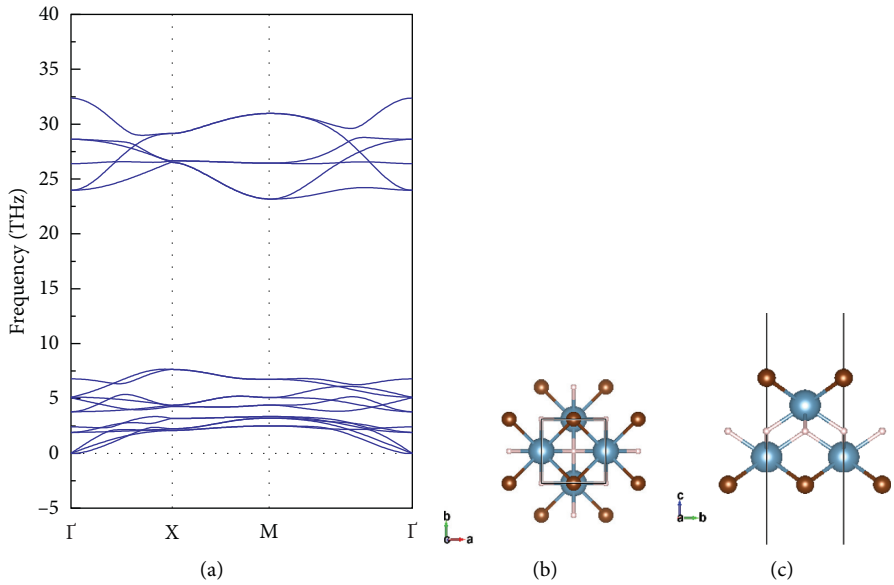

Figure 2: (a) The calculated phonon dispersion curves of monolayer CaHBr. (b) and (c) Main view and side view of primitive unit cell of monolayer CaHBr.

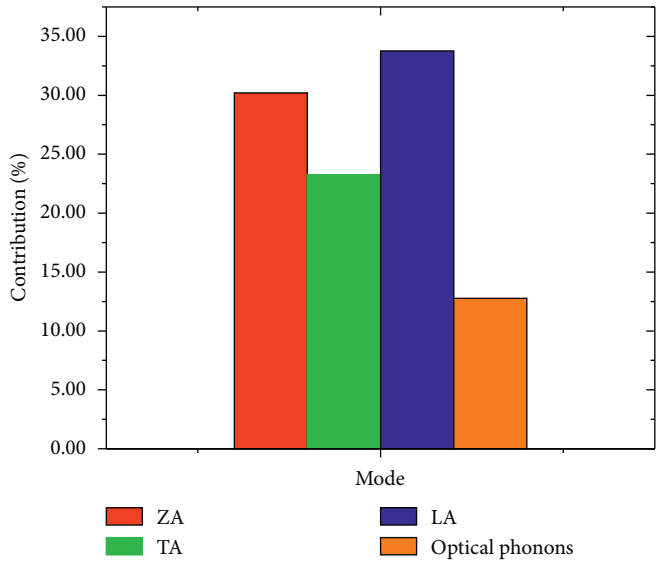

Figure 3: Contributions of phonon modes to total lattice thermal conductivity, where the red bars represent the ZA branches of acoustics, the green bars represent the TA branches of acoustics, the blue bars represent the LA branches of acoustics, and the orange bars represent the optical branches.

between the cumulative lattice thermal conductivity and the maximum mean free path (MFP) Λ_{max} at room temperature. When drawing a curve with a logarithmic scale as the horizontal axis, we can find the similarity of the curve to a logistic function, indicating that the form is suitable for the following nonparametric function:

$$\kappa_l(\Lambda \leq \Lambda_{max}) = \frac{\kappa_l}{1 + (\Lambda_0/\Lambda_{max}).} \quad (7)$$

It is found from Figure 6 that the acoustic phonons with a length of 0–3.5 nm contribute to the thermal conductivity, while the optical phonons larger than 3.5 nm contribute little to the thermal conductivity.

For the efficiency and reliability of devices, the thermal transport property of materials is very important. At present, there are no experimental data and theoretical data for the thermal conductivity of the monolayer CaHBr. By testing the sensitivity of the thermal conductivity to the temperature, the functional relationship between the lattice thermal conductivity and the temperature can be obtained in Figure 7, where we show the lattice thermal conductivities κ_l of the monolayer CaHBr in the temperatures ranging from

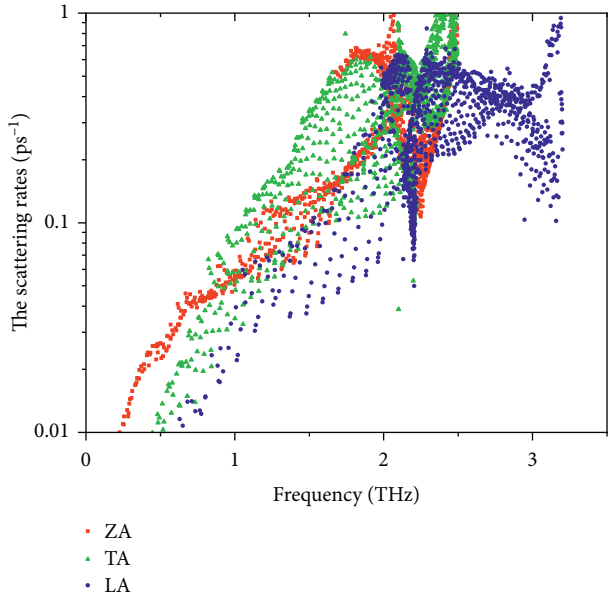

Figure 4: The phonon scattering rates of monolayer CaHBr at room temperature. The red squares (ZA), green triangles (TA), and blue circles (LA) are the acoustic modes.

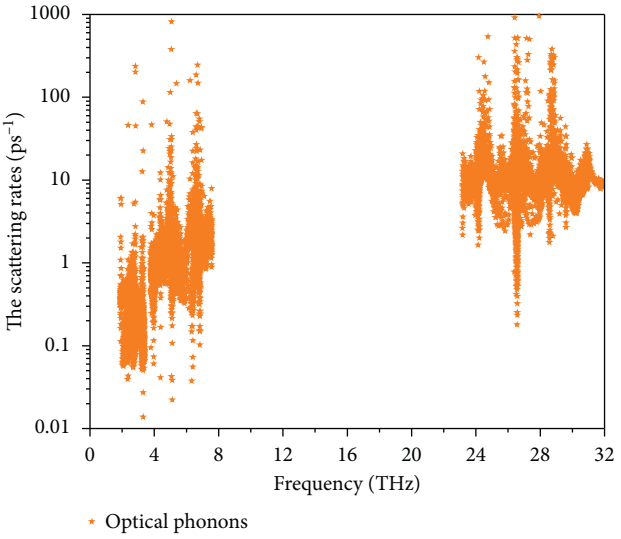

Figure 5: The phonon scattering rates of monolayer CaHBr at room temperature. The orange star is for the optic modes.

30 K to 1200 K with a $94 \times 94 \times 1$ k-grid in the scalebroad = 1.0. It can be seen that the lattice thermal conductivity increases exponentially with the increase of temperature T at low temperatures and tends to be proportional to $1/T$ at high temperatures. The lattice thermal conductivity of monolayer CaHBr at room temperature is 2.469 W/m · K and 2.201 W/m · K for BTE and RTA, respectively.

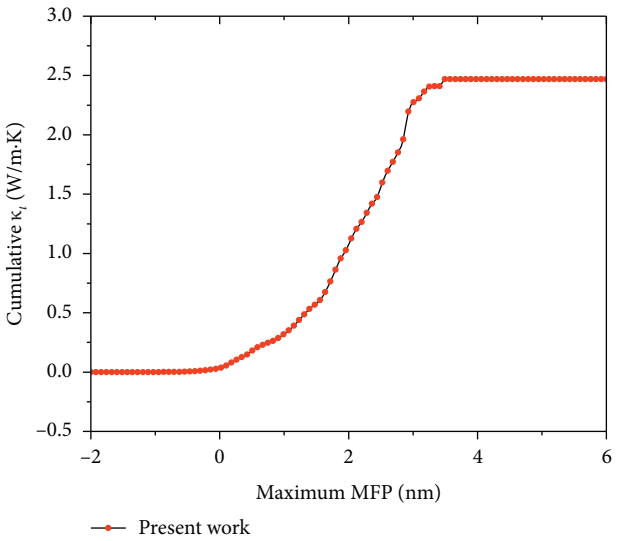

Figure 6: Calculated cumulative thermal conductivity of monolayer CaHBr as a function of maximum mean free path (MFP) at room temperature.

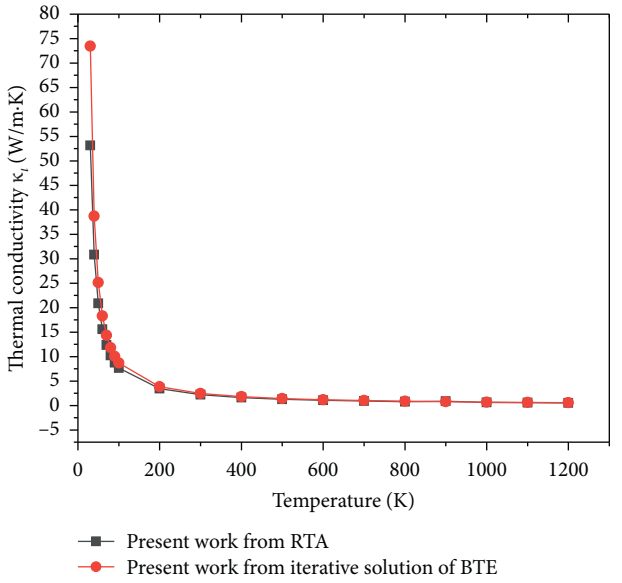

Figure 7: Lattice thermal conductivity κ_l of monolayer CaHBr at different temperatures ranging from 30 K to 1200 K. Black squares, our results from RTA; red circles, our results from iterative solution of BTE with scalebroad = 1.0.

4. Conclusions

Based on density functional theory and Boltzmann transport equation, we study the structure, elastic properties, and lattice thermal conductivity of the monolayer CaHBr. The obtained equilibrium lattice constant $a = 3.843$ Å is well

consistent with another theoretical value $a = 3.829$ Å. The mechanical and thermodynamic stability of monolayer CaHBr is proved by the obtained elastic properties and phonon spectra without imaginary frequency. And the elastic limit of monolayer CaHBr is obtained by biaxial tensile strain. The second-order and third-order interatomic force constants are obtained by using the finite difference method. The thermal conductivity of the monolayer CaHBr at room temperature is 2.469 W/m · K and 2.201 W/m · K, respectively, by BTE and RTA iterations. The two methods can obtain good results for the calculation of thermal conductivity of monolayer CaHBr. It can be seen that the lattice thermal conductivity of the obtained monolayer CaHBr is low, and the result shows that the lattice thermal conductivity mainly depends on the acoustic modes. We hope that our results can provide theoretical guidance for the experimental exploration and application of the relevant properties of layered monolayer CaHBr.

Data Availability

The data used to support the findings of this study are included within the article.

Conflicts of Interest

The authors declare that they have no known conflicts of interest.

Acknowledgments

This work was supported by the Guizhou Sci-Tech Fund of China (Grant No. [2017] 1125). The authors also acknowledge the support for the computational resources by the Chinese Academy of Engineering Physics and the State Key Laboratory of Polymer Materials Engineering of China in Sichuan University.

References

[1] Z. Sun and H. Chang, "Graphene and graphene-like two-dimensional materials in photodetection: mechanisms and methodology," *ACS Nano*, vol. 8, no. 5, pp. 4133–4156, 2014.

[2] X. Tong, H. Cheng, and R. Zeng, "Synthesis of graphene nanosheets via hydrogen reduction of thermal exfoliated graphite oxide," *Materials Review*, vol. 45, no. 7, pp. 1558–1565, 2014.

[3] A. Gupta, T. Sakthivel, and S. Seal, "Recent development in 2D materials beyond graphene," *Progress in Materials Science*, vol. 73, pp. 44–126, 2015.

[4] S. Z. Butler, S. M. Hollen, L. Cao et al., "Progress, challenges, and opportunities in two-dimensional materials beyond graphene," *ACS Nano*, vol. 7, no. 4, pp. 2898–2926, 2013.

[5] R. Buchanan, "Introduction to graphene special edition," *Journal of Applied Toxicology*, vol. 37, no. 11, pp. 1286-1287, 2017.

[6] F. Pulizzi, O. Bubnova, S. Milana, D. Schilter, D. Abergel, and A. Moscatelli, "Graphene in the making," *Nature Nanotechnology*, vol. 14, no. 10, pp. 914–918, 2019.

[7] A. Bablich, S. Kataria, and M. C. Lemme, "Graphene and two-dimensional materials for optoelectronic applications," *Electronics*, vol. 5, no. 13, 2016.

[8] S. Ulstrup, A. G. Čabo, J. A. Miwa et al., "Ultrafast band structure control of a two-dimensional heterostructure," *ACS Nano*, vol. 10, no. 6, pp. 6315–6322, 2016.

[9] J. Tao, T. Luttrell, and M. Batzill, "A two-dimensional phase of TiO2 with a reduced bandgap," *Nature Chemistry*, vol. 3, no. 4, pp. 296–300, 2011.

[10] S. J. Kim, K. Choi, B. Lee, Y. Kim, and B. H. Hong, "Materials for flexible, stretchable electronics: graphene and 2D materials," *Annual Review of Materials Research*, vol. 45, no. 1, pp. 63–84, 2015.

[11] A. A. Balandin, S. Ghosh, W. Bao et al., "Superior thermal conductivity of single-layer graphene," *Nano Letters*, vol. 8, no. 3, pp. 902–907, 2008.

[12] M. de Castro Vítores, R. Candori, F. Pirani, V. Aquilanti, M. Garay, and A. González Ureña, "Determination of D00 (Ca. . .HBr) from full and half collision studies. Van der Waals and charge transfer contributions to the formation of Ca. . .HX (X = Cl, Br) complexes," *Chemical Physics Letters*, vol. 263, no. 3-4, pp. 456–462, 1996.

[13] C. V. Vishnu Vardhan, S. Ghosh, S. Nagaraj, R. Sridharan, and T. Gnanasekaran, "Phase diagram study of CaBr2-CaHBr system," *Journal of Thermal Analysis And Calorimetry*, vol. 112, no. 1, pp. 127–131, 2013.

[14] P. Ehrlich, B. Alt, and L. Gentsch, "Uber die Hydridchloride der Erdalkalimetalle," *Zeitschrift fur anorganische und allgemeine Chemie*, vol. 283, no. 1-6, p. 58, 1956.

[15] S. S. Kumar, S. Ghosh, M. Sahu, and R. Ganesan, "Molar heat capacity measurement of CaHCl and CaHBr," *Journal of Chemical Sciences*, vol. 131, no. 9, p. 100, 2019.

[16] G. Qin, Z. Qin, S.-Y. Yue, Q.-B. Yan, and M. Hu, "External electric field driving the ultra-low thermal conductivity of silicene," *Nanoscale*, vol. 9, no. 21, p. 7227, 2017.

[17] H. Wang, G. Qin, G. Li, Q. Wang, and M. Hu, "Low thermal conductivity of monolayer ZnO and its anomalous temperature dependence," *Physical Chemistry Chemical Physics*, vol. 19, no. 20, p. 12882, 2017.

[18] G. Qin, Z. Qin, H. Wang, and M. Hu, "Lone-pair electrons induced anomalous enhancement of thermal transport in strained planar two-dimensional materials," *Nano Energy*, vol. 50, p. 425, 2018.

[19] H. Liu, G. Qin, Y. Lin, and M. Hu, "Disparate strain dependent thermal conductivity of two-dimensional penta-structures," *Nano Letters*, vol. 16, no. 6, p. 3831, 2016.

[20] R. Peierls, "Zur kinetischen theorie der Wärmeleitung in kristallen," *Annalen der Physik*, vol. 395, no. 8, pp. 1055–1101, 1929.

[21] M. Omini and A. Sparavigna, "Beyond the isotropic-model approximation in the theory of thermal conductivity," *Physical Review B*, vol. 53, no. 14, pp. 9064–9073, 1996.

[22] J. M. Ziman, *Electrons and Phonons*, Oxford University Press, London, UK, 1960.

[23] J. Callaway, "Model for lattice thermal conductivity at low temperatures," *Physical Review*, vol. 113, no. 4, pp. 1046–1051, 1959.

[24] P. B. Allen, "Improved callaway model for lattice thermal conductivity," *Physical Review B*, vol. 88, Article ID 144302, 2013.

[25] C. He, C.-E. Hu, T. Zhang, Y.-Y. Qi, and X.-R. Chen, "Lattice dynamics and thermal conductivity of cesium chloride via first-principles investigation," *Solid State Communications*, vol. 254, pp. 31–36, 2017.

[26] W. Li, J. Carrete, N. A. Katcho, and N. Mingo, "ShengBTE: a solver of the Boltzmann transport equation for phonons," *Computer Physics Communications*, vol. 185, no. 6, pp. 1747–1758, 2014.

[27] R. A. Cowley, "The lattice dynamics of an anharmonic crystal," *Advances in Physics*, vol. 12, no. 48, pp. 421–480, 1963.

[28] N. Guo, K. M. Yam, and C. Zhang, "Light controllable catalytic activity of Au clusters decorated with photochromic molecules," *Nanotechnology*, vol. 29, no. 24, Article ID 245705, 2018.

[29] N. Guo, K. M. Yam, X. L. Wang, and C. Zhang, "N-doped ZnO nanosheets: towards high performance two dimensional catalysts," *Nanotechnology*, vol. 29, no. 10, Article ID 105707, 2018.

[30] Y. Zhou, Y.-Q. Zhao, Z.-Y. Zeng, X.-R. Chen, and H.-Y. Geng, "Anisotropic thermoelectric properties of Weyl semimetal NbX (X = P and As): a potential thermoelectric material," *Physical Chemistry Chemical Physics*, vol. 21, no. 27, p. 15167, 2019.

[31] Y. Zhou, W. L. Tao, Z. Y. Zeng, X. R. Chen, and Q. F. Chen, "Thermoelectric properties of topological insulator lanthanum phosphide via first-principles study," *Journal of Applied Physics*, vol. 125, no. 4, Article ID 045107, 2019.

[32] X. L. Pan, Y. Q. Zhao, Z. Y. Zeng, X. R. Chen, and Q. F. Chen, "Electronic, elastic, optical and thermal transport properties of penta-PdAs2 monolayer: first-principles study," *Solid State Communications*, vol. 307, Article ID 113802, 2020.

[33] X.-F. Chen, L. Wang, Z.-Y. Zeng, X.-R. Chen, and Q.-F. Chen, "Strain-tunable electronic, elastic, and optical properties of CaI2 monolayer: first-principles study," *Philosophical Magazine*, vol. 100, no. 15, pp. 1982–2000, 2020.

[34] P. E. Blöchl, "Projector augmented-wave method," *Physical Review B*, vol. 50, no. 24, p. 17953, 1994.

[35] G. Kresse and J. Furthmüller, "Efficient iterative schemes forab initiototal-energy calculations using a plane-wave basis set," *Physical Review B*, vol. 54, no. 16, pp. 11169–11186, 1996.

[36] J. P. Perdew, K. Burke, and M. Ernzerhof, "Generalized gradient approximation made simple," *Physical Review Letters*, vol. 77, no. 18, pp. 3865–3868, 1996.

[37] S. H. Vosko, L. Wilk, and M. Nusair, "Accurate spin-dependent electron liquid correlation energies for local spin density calculations: a critical analysis," *Canadian Journal of Physics*, vol. 58, no. 8, p. 1200, 1980.

[38] N. Mounet, M. Gibertini, P. Schwaller et al., "Two-dimensional materials from high-throughput computational exfoliation of experimentally known compounds," *Nature Nanotechnology*, vol. 13, no. 3, pp. 246–252, 2018.

[39] Y. Lu, Y. Yang, F. Zheng, B.-T. Wang, and P. Zhang, "Electronic, mechanical, and thermodynamic properties of americium dioxide," *Journal of Nuclear Materials*, vol. 441, no. 1-3, pp. 411–420, 2013.

[40] P. Lab Guerie, F. Pascale, M. M Rawa, C. Zicovich-Wilson, N. Makhouki, and R. Dovesi, "Phonon vibrational frequencies and elastic properties of solid SrFCl. An ab initio study," *The European Physical Journal B*, vol. 43, no. 4, pp. 453–461, 2005.

[41] M. Mérawa, Y. Noël, B. Civalleri, R. Brown, and R. Dovesi, "Raman and infrared vibrational frequencies and elastic properties of solid BaFCl calculated with various Hamiltonians: anab initiostudy," *Journal of Physics: Condensed Matter*, vol. 17, no. 3, p. 535, 2005.

[42] R. Ran, C. Cheng, Z.-Y. Zeng, X.-R. Chen, and Q.-F. Chen, "Mechanical and thermal transport properties of monolayer PbI2 via first-principles investigations," *Philosophical Magazine*, vol. 99, no. 10, pp. 1277–1296, 2019.

[43] R. C. Andrew, R. E. Mapasha, A. M. Ukpong, and N. Chetty, "Mechanical properties of graphene and boronitrene," *Physical Review B: Condensed Matter and Materials Physics*, vol. 85, no. 12, Article ID 125428, 2012.

[44] Z. Zhang and W. Guo, "Intrinsic metallic and semiconducting cubic boron nitride nanofilms," *Nano Letters*, vol. 12, no. 7, pp. 3650–3655, 2012.

[45] F. Mouhat and F. Coudert, "Necessary and sufficient elastic stability conditions in various crystal systems," *Physical Review B: Condensed Matter and Materials Physics*, vol. 90, no. 22, Article ID 224104, 2014.

[46] H. Peelaers and C. G. Van de Walle, "Elastic constants and pressure-induced effects in MoS_2," *The Journal of Physical Chemistry C*, vol. 118, no. 22, p. 12073, 2014.

[47] T. Liang, W.-Q. Chen, C.-E. Hu, X.-R. Chen, and Q.-F. Chen, "Lattice dynamics and thermal conductivity of lithium fluoride via first-principles calculations," *Solid State Communications*, vol. 272, pp. 28–32, 2018.

[48] X. Y. Hou, Y. Cheng, C. E. Hu, C. G. Piao, and H. Y. Geng, "Thermoelectric properties of strontium sulfide via first principles calculations," *Solid State Communications*, vol. 305, Article ID 113755, 2020.